Received: 29 June 2023 | Accepted: 20 September 2023

DOI: 10.1002/pamm.202300082

PAMM Proceedings in Applied Mathematics and Mechanics

RESEARCH ARTICLE

Approximate postbuckling analysis of shear deformable laminates

Jakob Christian Schilling | **Christian Mittelstedt**

Department of Mechanical Engineering, Institute for Lightweight Engineering and Structural Mechanics, Technical University of Darmstadt, Darmstadt, Germany

Correspondence
Jakob Christian Schilling, Department of Mechanical Engineering, Institute for Lightweight Engineering and Structural Mechanics, Technical University of Darmstadt, Otto-Berndt-Str. 2, 64287 Darmstadt, Germany.
Email:
jakob.schilling@klub.tu-darmstadt.de

Funding information
German Research Foundation,
Grant/Award Number: 426146527

Abstract
In the lightweight design of aircraft, spacecraft and marine vessels, often advanced materials are utilised. Advanced materials such as laminated composites made of fibre-reinforced plastics show transverse shear deformations if they are considered "thick" or possess little transverse shear stiffness. In most cases, the effect of the shear deformations is neglected, and few computational models exist that consider the closed-form approximate analysis of the postbuckling behaviour. Thus, a new computational model based on high-order shear deformation theories is introduced. The solution is derived based on the principle of the minimum of the total elastic potential and is evaluated in comparison to finite element analyses. The highly efficient approximate computational model is developed to offer a valuable tool for the preliminary design of lightweight structures utilising shear deformable advanced materials.

1 | INTRODUCTION

Composite laminates made of fibre-reinforced plastics are frequently used for example in the aerospace, marine and civil engineering industry. Here, they are important for the lightweight design of structures because of their advantageous material properties that offer high specific strength and stiffness. However, the transverse shear stiffness is low compared to other commonly used materials. Typically, laminated plates are analysed using the classical laminated plate theory (CLPT), which does not model shear deformation effects. For thick laminated plates or plates with very low transverse shear stiffness, this simplification leads to an overestimation of the load-carrying capabilities, that is, critical buckling loads are overestimated [1]. Consequently, also the postbuckling behaviour is affected.

For the analysis of shear deformable laminates, shear deformation theories (SDT), such as the first-order shear deformation (FSDT) and third-order shear deformation theory (TSDT), are required. The description of the constitutive behaviour in the present work is based on the TSDT as formulated by Reddy [2], as it does not require a shear correction factor and fulfills the boundary condition of vanishing transverse shear stresses at the top and bottom surface of the laminate. This is contrary to the FSDT. The utilisation of the TSDT leads to two additional degrees of freedom, which are the independent rotations of the transverse cross-sections ψ_x and ψ_y.

A crucial factor in the lightweight design of structures is the stability behaviour. In general, this behaviour can be analysed using various analytical and numerical methods, such as the finite-element method, the finite strip method, the semi-analytical Ritz method and closed-from analytical solutions. For the preliminary design, when for example,

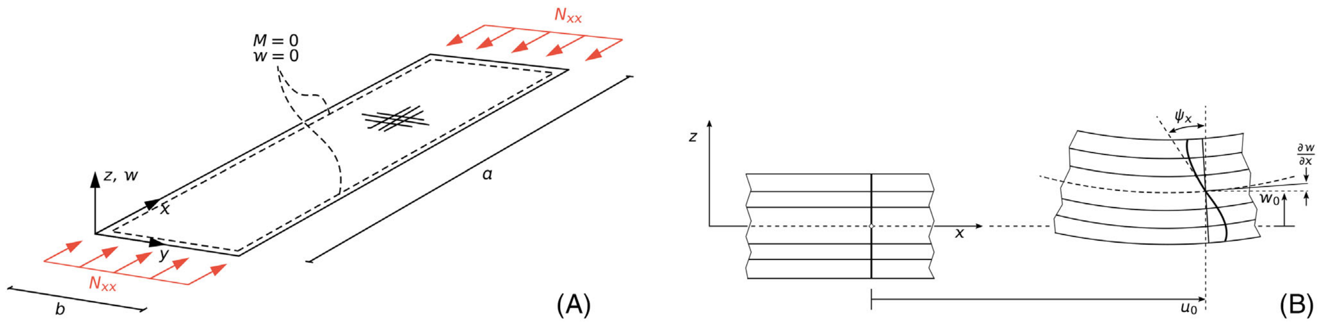

FIGURE 1 (A) Simply supported laminated plate under uniaxial compression. (B) Sketch of the deformed and undeformed laminated panel in the xz-plane with the mid-plane deflection w_0, the in-plane displacement u_0, the slope $\frac{\partial w_0}{\partial x}$ and the rotation ψ_x.

an optimisation is performed to fully exploit the lightweight potential, computational efficiency is a vital criterion for the selection of appropriate analysis tools. Due to the high number of function evaluations, the utilisation of closed-form analytical models is preferred. This is despite their often approximate character. Consequently, the present work is focused on the development of closed-form analytical solutions.

In the literature, the problem of buckling and postbuckling is addressed by numerous authors. Thus, the review of relevant literature is presented focused on closed-form modelling approaches for on the one-hand postbuckling of laminates based on CLPT and on the other-hand buckling of shear deformable laminates based on SDT. In most closed-form analytical models, the postbuckling analysis considers single laminated plates with varying boundary conditions [3–9]. This includes the modelling of uniaxially compressed cross-ply laminates with elastically restraint longitudinal edges [3], infinitely long panels under combined biaxial and shear loading including bending-twisting coupling [5], modelling of imperfect fully simply-supported (SSSS) and combined simply-supported and clamped (SSCC) panels [8], and other combinations of the listed boundary and loading conditions. However, also more complex structures are investigated in a closed-form analytical fashion. Models for the postbuckling analysis are available for blade-stiffened [10] and omega-stringer-stiffened [11] composite panels. For a more extensive review of previous works regarding the postbuckling of laminated structures based on the CLPT, the reader is referred to Ref. [11]. For closed-form analytical analysis models based on FSDT or TSDT, no works are known to the authors that consider postbuckling. However, for the buckling analysis, several relevant works exist that investigate individual laminated panels with various boundary conditions. This includes next to the classical Navier solutions, for example, presented in Ref. [2], the consideration of SRSR panels based on FSDT [12] and based on TSDT [13–15]. A more detailed literature review is available in Ref. [16], where closed-form modelling approaches are presented for unsymmetrically laminated shear deformable laminates. From the review of relevant literature, a clear lack of computationally highly efficient analysis models for the postbuckling of shear deformable laminates is identified and addressed in the present work by extending the postbuckling models based on CLPT to the TSDT employing the insights gained by the modelling approaches for the buckling analyses.

The lack of fast analytical models is addressed in the present work by establishing a novel closed-form analytical postbuckling analysis model for a shear deformable panel with simply supported boundary conditions. The panel is depicted in Figure 1A. The approximate solution is derived based on the principle of the minimum of the total elastic potential. Therefore, the total elastic potential energy is derived based on the TSDT and von Kármán strains, including initial imperfections of the panel. The equilibrium conditions are reduced by using a suitable Airy stress function. First, a linear buckling solution is derived and used as the starting point for a consecutively derived nonlinear postbuckling solution. The results of the novel approach are successfully verified against finite-element analyses and show promising potential for their future application in preliminary design.

2 | METHODS

2.1 | Introduction

Before suitable shape functions for the buckling pattern are selected, the constitutive and kinematic relations are defined. The present approach is based on the TSDT. For brevity, the reader is referred to standard textbooks [2, 4] for the detailed description of the constitutive relationship for laminates based on the TSDT. The foundation of the TSDT is the assumption of a displacement field that effectively reduces the multilayered structure to an equivalent single layer. Thus, the displacements u, v and w are described by the laminate's mid-plane displacements u_0, v_0 and w_0. The displacement field is given in Equation (1).

$$u(x,y,z) = u_0(x,y) + z\,\psi_x(x,y) - \frac{4\,z^3}{3\,h^2}\left(\psi_x + \frac{\partial w_0(x,y)}{\partial x}\right) \tag{1}$$

$$v(x,y,z) = v_0(x,y) + z\,\psi_y(x,y) - \frac{4\,z^3}{3\,h^2}\left(\psi_y + \frac{\partial w_0(x,y)}{\partial y}\right) \tag{2}$$

$$w(x,y) = w_0(x,y) \tag{3}$$

Note that the additional degrees of freedom ψ_x and ψ_y are included in the formulation. The deformation is additionally graphically represented in Figure 1B. Inserting the displacement field into the von Kármán strains leads to the strain formulation in Equations (4–5) based on the TSDT required for the computation of the total elastic potential. However, to include imperfections in the formulation the deflection w is substituted with $w(x,\ y) = w_0(x,\ y) + w_\mathrm{i}(x,\ y)$.

$$\underline{\epsilon}^{(0)} = \begin{pmatrix} \frac{\partial u_0}{\partial x} + \frac{1}{2}\left(\frac{\partial w_0}{\partial x}\right)^2 + \frac{\partial w_i}{\partial x}\frac{\partial w_0}{\partial x} \\ \frac{\partial v_0}{\partial y} + \frac{1}{2}\left(\frac{\partial w_0}{\partial y}\right)^2 + \frac{\partial w_i}{\partial y}\frac{\partial w_0}{\partial y} \\ \frac{\partial u_0}{\partial y} + \frac{\partial v_0}{\partial x} + \frac{\partial w_0}{\partial y}\frac{\partial w_0}{\partial x} + \frac{\partial w_i}{\partial y}\frac{\partial w_0}{\partial x} + \frac{\partial w_0}{\partial y}\frac{\partial w_i}{\partial x} \end{pmatrix} \qquad \underline{\epsilon}^{(1)} = \begin{pmatrix} \frac{\partial \psi_x}{\partial x} \\ \frac{\partial \psi_y}{\partial y} \\ \frac{\partial \psi_y}{\partial x} + \frac{\partial \psi_x}{\partial y} \end{pmatrix} \tag{4}$$

$$\underline{\epsilon}^{(3)} = -\frac{4}{3\,h^2}\begin{pmatrix} \frac{\partial \psi_x}{\partial x} + \frac{\partial^2 w_0}{\partial x^2} \\ \frac{\partial \psi_y}{\partial y} + \frac{\partial^2 w_0}{\partial y^2} \\ \frac{\partial \psi_y}{\partial x} + \frac{\partial \psi_x}{\partial y} + 2\,\frac{\partial^2 w_0}{\partial x \partial y} \end{pmatrix} \qquad \underline{\gamma}^{(0)} = \begin{pmatrix} \frac{\partial w_0}{\partial y} + \psi_y \\ \frac{\partial w_0}{\partial x} + \psi_x \end{pmatrix} \qquad \underline{\gamma}^{(2)} = -\frac{4}{h^2}\begin{pmatrix} \frac{\partial w_0}{\partial y} + \psi_y \\ \frac{\partial w_0}{\partial x} + \psi_x \end{pmatrix} \tag{5}$$

The following terms of the derivations of the imperfection w_i are neglected:

$$\left(\frac{\partial w_i}{\partial x}\right)^2,\ \left(\frac{\partial w_i}{\partial y}\right)^2,\ \frac{\partial w_i}{\partial x}\frac{\partial w_i}{\partial y},\ \frac{\partial^2 w_i}{\partial x^2},\ \frac{\partial^2 w_i}{\partial y^2},\ \frac{\partial^2 w_i}{\partial x \partial y},\ \frac{\partial w_\mathrm{i}}{\partial x} \text{ in } \underline{\gamma}^{(0,2)},\ \frac{\partial w_\mathrm{i}}{\partial y} \text{ in } \underline{\gamma}^{(0,2)}$$

In short, the constitutive relationship can be given as follows in Equation (6).

$$\begin{Bmatrix} \underline{N}^0 \\ \underline{M}^0 \\ \underline{P} \\ \underline{Q} \\ \underline{R} \end{Bmatrix} = \begin{bmatrix} \underline{\underline{A}} & \underline{\underline{B}} & \underline{\underline{E}} & \underline{\underline{0}} & \underline{\underline{0}} \\ \underline{\underline{B}} & \underline{\underline{D}} & \underline{\underline{F}} & \underline{\underline{0}} & \underline{\underline{0}} \\ \underline{\underline{E}} & \underline{\underline{F}} & \underline{\underline{H}} & \underline{\underline{0}} & \underline{\underline{0}} \\ \underline{\underline{0}} & \underline{\underline{0}} & \underline{\underline{0}} & \underline{\underline{A}}_\mathrm{S} & \underline{\underline{D}}_\mathrm{S} \\ \underline{\underline{0}} & \underline{\underline{0}} & \underline{\underline{0}} & \underline{\underline{D}}_\mathrm{S} & \underline{\underline{F}}_\mathrm{S} \end{bmatrix} \begin{Bmatrix} \underline{\epsilon}^{(0)} \\ \underline{\epsilon}^{(1)} \\ \underline{\epsilon}^{(3)} \\ \underline{\gamma}^{(0)} \\ \underline{\gamma}^{(2)} \end{Bmatrix} \tag{6}$$

For the description of the postbuckling problem, not only the strains and constitutive relations but also the equilibrium conditions are necessary. They are presented based on the TSDT in Equations (7–10).

$$\frac{\partial N^0_{xx}}{\partial x} + \frac{\partial N^0_{xy}}{\partial y} = 0 \qquad \frac{\partial N^0_{xy}}{\partial x} + \frac{\partial N^0_{yy}}{\partial y} = 0 \tag{7}$$

$$\frac{\partial M^0_{xx}}{\partial x} + \frac{\partial M^0_{xy}}{\partial y} - \frac{4}{3h^2}\left(\frac{\partial P_{xx}}{\partial x} + \frac{\partial P_{xy}}{\partial y}\right) + \frac{4\,R_x}{h^2} = Q_x \tag{8}$$

$$\frac{\partial M^0_{xy}}{\partial x} + \frac{\partial M^0_{yy}}{\partial y} - \frac{4}{3h^2}\left(\frac{\partial P_{xy}}{\partial x} + \frac{\partial P_{yy}}{\partial y}\right) + \frac{4\,R_y}{h^2} = Q_y \tag{9}$$

$$\frac{\partial Q_x}{\partial x} + \frac{\partial Q_y}{\partial y} - \frac{4}{h^2}\left(\frac{\partial R_x}{\partial x} + \frac{\partial R_y}{\partial y}\right) + \frac{4}{3h^2}\left(\frac{\partial^2 P_{xx}}{\partial x^2} + \frac{\partial^2 P_x y}{\partial x \partial y} + \frac{\partial^2 P_{yy}}{\partial y^2}\right) = 0 \tag{10}$$

The five partial differential equations are consecutively reduced to a set of four by introducing an Airy stress function. The buckling pattern is represented by a set of trigonometric buckling shape functions that is given in Equations (11–12). The functions fulfill the required boundary conditions of a simply supported panel. Thus, they can be considered to be suitable shape functions.

$$w_0 = W\,\sin\left(\frac{\pi\, m\, x}{a}\right)\,\sin\left(\frac{\pi\, n\, y}{b}\right) \tag{11}$$

$$\psi_x = X\,\frac{\pi\, m}{a}\,\cos\left(\frac{\pi\, m\, x}{a}\right)\,\sin\left(\frac{\pi\, n\, y}{b}\right) \qquad \psi_y = Y\,\frac{\pi\, n}{b}\,\cos\left(\frac{\pi\, n\, y}{b}\right)\,\sin\left(\frac{\pi\, m\, x}{a}\right) \tag{12}$$

2.2 | Airy stress function

The Airy stress function θ is chosen to define the in-plane force resultants N^0_{xx}, N^0_{yy} and N^0_{xy} to fulfil the equilibrium conditions (7). This leads to the formulation given in Equation (13).

$$N^0_{xx} = \frac{\partial^2 \theta}{\partial y^2} \qquad N^0_{yy} = \frac{\partial^2 \theta}{\partial x^2} \qquad N^0_{xy} = -\frac{\partial^2 \theta}{\partial x \partial y} \tag{13}$$

By formulating a semi-inverse representation of the constitutive law, where the decoupled in-plane strains are expressed depending on the in-plane force resultants, the following formulation for the strains is reached, depending on the inverse membrane stiffnesses $\bar{A}_{ij}$.

$$\epsilon^0_{xx} = \bar{A}_{12}\,\frac{\partial^2}{\partial x^2}\,\theta + \bar{A}_{11}\,\frac{\partial^2}{\partial y^2}\,\theta \qquad \epsilon^0_{yy} = \bar{A}_{22}\,\frac{\partial^2}{\partial x^2}\,\theta + \bar{A}_{12}\,\frac{\partial^2}{\partial y^2}\,\theta \qquad \gamma^0_{xy} = -\bar{A}_{66}\,\frac{\partial}{\partial y}\,\frac{\partial}{\partial x}\,\theta \tag{14}$$

Considering the necessary compatibility of the in-plane strains as given in Equation (15), an additional partial differential equation is formulated by expressing compatibility in the form of strains given in Equation (14) and based on the von Kármán strains for the TSDT (Equations (4–5)).

$$\frac{\partial^2 \epsilon^0_{xx}}{\partial y^2} + \frac{\partial^2 \epsilon^0_{yy}}{\partial x^2} - \frac{\partial^2 \gamma^0_{xy}}{\partial x \partial y} = 0 \tag{15}$$

Hence, the compatibility equation is formulated in Equation (16).

$$\begin{aligned}
&\bar{A}_{22}\,\frac{\partial^4 \theta}{\partial x^4} + 2\,\bar{A}_{12}\,\frac{\partial^4 \theta}{\partial x^2 \partial y^2} + \bar{A}_{66}\,\frac{\partial^2 \theta}{\partial y^2 \partial x^2} + \bar{A}_{11}\,\frac{\partial^4 \theta}{\partial y^4} \\
&= \left(\frac{\partial^2 w_0}{\partial x \partial y}\right)^2 - \frac{\partial^2 w_0}{\partial x^2}\frac{\partial^2 w_0}{\partial y^2} - \frac{\partial^2 w_0}{\partial x^2}\frac{\partial^2 w_i}{\partial y^2} + 2\,\frac{\partial^2 w_0}{\partial x \partial y}\frac{\partial^2 w_i}{\partial x \partial y} - \frac{\partial^2 w_i}{\partial x^2}\frac{\partial^2 w_0}{\partial y^2}
\end{aligned} \tag{16}$$

where

$$\bar{A}_{11} = \frac{A_{22}}{A_{11}A_{22} - A_{12}^2},\ \bar{A}_{22} = \frac{A_{11}}{A_{11}A_{22} - A_{12}^2},\ \bar{A}_{12} = \frac{A_{12}}{A_{12}^2 - A_{11}A_{22}},\ \bar{A}_{66} = \frac{1}{A_{66}}$$

It can be noted that the imperfections w_i are included in the given representation. The compatibility equation is solved, obtaining a particular and homogeneous solution for the Airy stress function. Using a suitable ansatz, the particular solution θ_p is obtained after inserting the buckling shape function w_0 and imperfection w_i by comparison of coefficients. The resulting expression is given in Equation (17).

The homogeneous solution is responsible for taking the in-plane boundary conditions into account. As the requirements of straight and shear force free longitudinal edges are automatically fulfilled by the chosen set of buckling shape functions, only the applied loading is introduced as formulated in Equation (17)

$$\theta_h = N_{xx}\frac{y^2}{2} \qquad \theta_p = \left(W^2 + 2\,W\,W_\mathrm{i}\right)\left[\cos\left(\frac{\pi\,m\,x}{a}\right)^2 \frac{a^2\,n^2}{16\,\bar{A}_{22}\,b^2\,m^2} + \cos\left(\frac{\pi\,n\,y}{b}\right)^2 \frac{b^2\,m^2}{16\,\bar{A}_{11}\,a^2\,n^2}\right] \tag{17}$$

The complete airy stress function is consequently obtained by the sum of the two contributions.

2.3 | Total elastic potential

With the fully defined Airy stress function, the defined set of buckling shape functions, and the initial imperfection, the total elastic potential Π can be computed. It consists of the contributions due to the membrane behaviour Π_m, the bending behaviour Π_b and the external forces Π_e which are formulated in Equations (18–19)

$$\Pi_\mathrm{m} = \frac{1}{2}\int\int \underline{N}^{0^T}\,\underline{\underline{\bar{A}}}\,\underline{N}^0\,dx\,dy \qquad \Pi_\mathrm{e} = \int_0^a\int_0^b -N_\mathrm{xx}\left(\bar{A}_{12}\frac{\partial^2}{\partial x^2}\theta(x,y) + \bar{A}_{11}\frac{\partial^2}{\partial y^2}\theta(x,y)\right)dx\,dy \tag{18}$$

$$\Pi_\mathrm{b} = \frac{1}{2}\int\int \begin{Bmatrix} \underline{\epsilon}^{(1)} \\ \underline{\epsilon}^{(3)} \\ \underline{\gamma}^{(0)} \\ \underline{\gamma}^{(2)} \end{Bmatrix}^T \begin{bmatrix} \underline{\underline{D}} & \underline{\underline{F}} & \underline{\underline{0}} & \underline{\underline{0}} \\ \underline{\underline{F}} & \underline{\underline{H}} & \underline{\underline{0}} & \underline{\underline{0}} \\ \underline{\underline{0}} & \underline{\underline{0}} & \underline{\underline{A}}_\mathrm{S} & \underline{\underline{D}}_\mathrm{S} \\ \underline{\underline{0}} & \underline{\underline{0}} & \underline{\underline{D}}_\mathrm{S} & \underline{\underline{F}}_\mathrm{S} \end{bmatrix} \begin{Bmatrix} \underline{\epsilon}^{(1)} \\ \underline{\epsilon}^{(3)} \\ \underline{\gamma}^{(0)} \\ \underline{\gamma}^{(2)} \end{Bmatrix} dx\,dy \qquad \underline{N}^{(0)} = \begin{Bmatrix} \frac{\partial^2\theta}{\partial y^2} \\ \frac{\partial^2\theta}{\partial x^2} \\ \frac{\partial^2\theta}{\partial x\partial y} \end{Bmatrix} \tag{19}$$

Thus, the total elastic potential is finally obtained as the sum of the three contributions and a function depending only on the unknowns $W,\ X$ and Y as shown in Equation (20)

$$\begin{aligned} \Pi(W,\,X,\,Y) = \Pi_\mathrm{m} + \Pi_\mathrm{b} + \Pi_\mathrm{e} = K_{e,2}\,{N_\mathrm{xx}}^2 + K_{m,3}\,{N_\mathrm{xx}}^2 + K_{b,8}\,W^2 + K_{b,1}\,X^2 + K_{b,5}Y^2 + K_{b,3}\,W\,X \\ + K_{e,1}\left(N_\mathrm{xx}\,W^2 + 2\,N_\mathrm{xx}\,W\,W_i\right) + K_{m,1}\left(W^4 + 4\,W^3\,W_i + 4\,W^2\,{W_i}^2\right) + K_{b,6}\,W\,Y + K_{b,2}\,X\,Y \end{aligned} \tag{20}$$

Here, the cofactors $K_{\mathrm{e},i}$, $K_{\mathrm{b},j}$ and $K_{\mathrm{m},h}$ are computed based on the buckling shape functions, the dimensions, and the material properties of the panel. Based on the total elastic potential, a solution for the linear buckling analysis and the postbuckling analysis is derived in the next subsections. Both utilise the principle of the minimum of the total elastic potential that leads to the formulation of three Ritz-equations (21).

$$\frac{\partial\Pi}{\partial W} = 0 \qquad \frac{\partial\Pi}{\partial X} = 0 \qquad \frac{\partial\Pi}{\partial Y} = 0 \tag{21}$$

2.4 | Buckling analysis

For the buckling analysis, the total elastic potential Π is simplified by omitting the expressions W^4 and W_i. This leads to the simplified expression in Equation (22).

$$\begin{aligned}\Pi_\mathrm{lin} = {} & K_{b,1}\,X^2 + K_{b,2}\,X\,Y + K_{b,3}\,W\,X + K_{b,5}\,Y^2 + K_{b,6}\,W\,Y + \left(K_{b,8} + K_{e,1}\,N_\mathrm{xx}\right)W^2 \\ & + \left(K_{e,2} + K_{m,3}\right){N_\mathrm{xx}}^2\end{aligned} \tag{22}$$

The linear eigenvalue problem is formulated by deriving the Ritz equations (see Equation (21)). This leads to the expression in Equation (23).

$$\left(\begin{bmatrix} 2\,K_{b,8} & K_{b,3} & K_{b,6} \\ K_{b,3} & 2\,K_{b,1} & K_{b,2} \\ K_{b,6} & K_{b,2} & 2\,K_{b,5} \end{bmatrix} + \begin{bmatrix} 2\,K_{e,1} & 0 & 0 \\ 0 & 0 & 0 \\ 0 & 0 & 0 \end{bmatrix} N_\mathrm{xx}\right)\begin{bmatrix} W \\ X \\ Y \end{bmatrix} = \begin{bmatrix} 0 \\ 0 \\ 0 \end{bmatrix} \tag{23}$$

After eliminating X and Y, the linear system of equations can be explicitly solved for the critical buckling load N_cr as given in Equation (24)

$$N_\mathrm{cr} = -\frac{-4\,K_{b,1}\,K_{b,5}\,K_{b,8} + K_{b,1}\,{K_{b,6}}^2 + {K_{b,2}}^2\,K_{b,8} - K_{b,2}\,K_{b,3}\,K_{b,6} + {K_{b,3}}^2\,K_{b,5}}{K_{e,1}\left(-4\,K_{b,1}\,K_{b,5} + {K_{b,2}}^2\right)} \tag{24}$$

Evaluating the solution for different half-wave numbers m, the critical value is obtained and is used as starting point for the postbuckling analysis.

2.5 | Postbuckling analysis

The postbuckling analysis is based on the total elastic potential as formulated in Equation (20). The nonlinear system of equations resulting from the Ritz-equations (21) allows again for the elimination of X and Y. This consequently leads to one single nonlinear Equation (25) that is solved for the postbuckling amplitude W.

$$\begin{aligned}&\left(-16\,K_{b,1}\,K_{b,5}\,K_{m,1} + 4\,{K_{b,2}}^2\,K_{m,1}\right)\left(W^3 + 3\,W^2\,W_i + 2\,W\,{W_i}^2\right) \\ &+ W\left(-8\,K_{b,1}\,K_{b,5}\,K_{b,8} + 2\,K_{b,1}\,{K_{b,6}}^2 + 2\,{K_{b,2}}^2\,K_{b,8} - 2\,K_{b,2}\,K_{b,3}\,K_{b,6} + 2\,{K_{b,3}}^2\,K_{b,5}\right) \\ &+ \left(N_\mathrm{xx}\,W + N_\mathrm{xx}\,W_i\right)\left(-8\,K_{b,1}\,K_{b,5}\,K_{e,1} + 2\,{K_{b,2}}^2\,K_{e,1}\right) = 0\end{aligned} \tag{25}$$

Introducing the substitute variables O_1, O_2 and O_3, the nonlinear equation is expressed in a simplified form in Equation (26).

$$W^3 + W^2\,O_1 + W\,O_2 + O_3 = 0 \tag{26}$$

For this nonlinear equation, an explicit solution for W is possible. With the defined amplitude W, the postbuckling behaviour can be described quantitatively. This includes the relationship between applied forces and the resulting displacements, resulting moments and forces, and the stress state in the laminate. Naturally, it is also possible to compute typical postbuckling parameters such as the effective width b_eff. The quality of the novel approximate solution is assessed in the next section in comparison with finite element analyses.

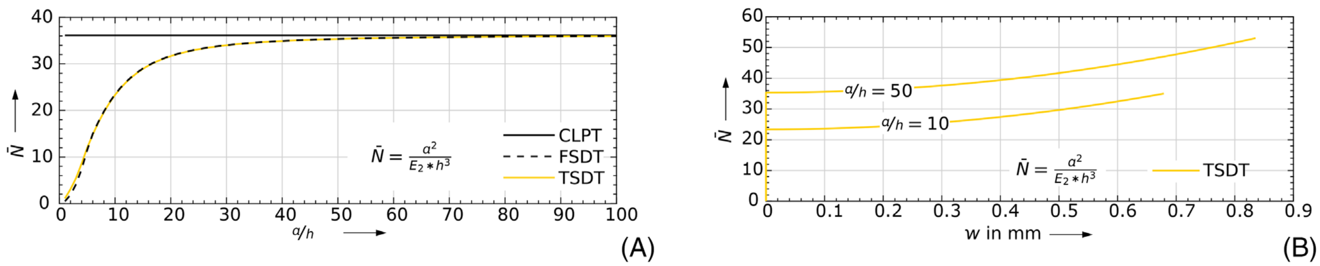

FIGURE 2 Influence of the thickness aspect ratios on: (A) the critical buckling load as obtained based on the CLPT, FSDT, and TSDT; (B) the postbuckling behaviour illustrated by load deflection curves for two selected exemplary thickness aspect ratios. TSDT, third-order shear deformation theory.

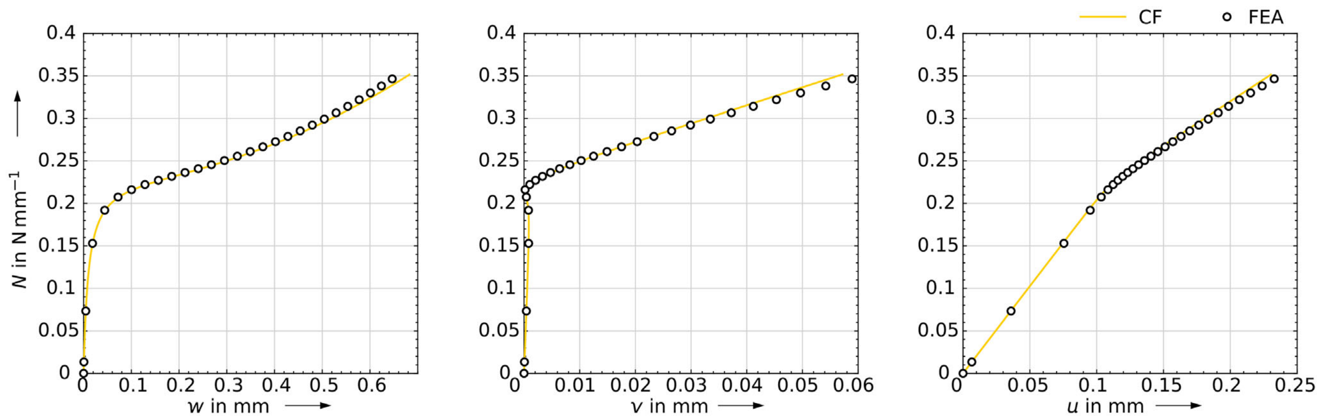

FIGURE 3 Applied loading N versus the displacements w, v, and u computed by the present closed-form analytical method (CF) and compared to results of finite element analysis.

3 | RESULTS AND DISCUSSION

The simply supported plate investigated in the present work is a cross-ply square laminate with four layers. The laminate configuration is proposed by Reddy [2] for the comparison of the different laminated plate theories (CLPT, FSDT, TSDT) and for this reason, adopted in the following investigation. The material of the single layer is defined with the ratio between the two elastic moduli E_1 and E_2, which is set to 40. The Poisson's ratio is 0.25. The shear moduli are assumed as $G_{12} = G_{13} = 0.6\,E_2$ and $G_{23} = 0.5\,E_2$. The elastic modulus E_2 is set to 1. The thickness aspect ratio is $a/h = 10$, if not stated otherwise.

Before the postbuckling behaviour is analysed, the buckling behaviour is investigated. The presented results clearly motivate the necessity of the utilisation of SDT for shear deformable laminates. In Figure 2A, the nondimensional critical buckling load is plotted based on the CLPT, FSDT, and TSDT versus the thickness aspect ratio a/h. It depicts the decrease of the critical buckling load due to the increasing thickness of the plate. Thus, the influence of shear deformation is not negligible. Because of this influence, also the postbuckling behaviour is affected, as illustrated in Figure 2B, where two exemplary load deflection curves are plotted for the thickness aspect ratios of $a/h = 10$ and $a/h = 50$. Considering the results in the two figures, the motivation to investigate shear deformable laminates is affirmed, as the influence on the buckling and postbuckling behaviour is clear. To assess the quality of the closed-form analytical solution, first, the behaviour of the displacements depending on the applied compressive loading is compared to finite element analysis in Figure 3. The load is evaluated for up to 1.5 times the critical buckling load. Consequently, the analysis considers only the early postbuckling regime. The agreement between the finite element analyses and the novel closed-form analytical model is very good for all three investigated displacements. The deviations become visible only for higher loads. It must be noted that also the initial imperfection is captured correctly by the analytical model. This is confirmed in Figure 4A, where the magnitude of the initial imperfection is varied from 0 to 0.02. The increasing imperfection results in increasing deflections in the area of the critical buckling load and significant deflections even before the bifurcation point of the perfect plate is reached. With increasing compression, the influence of the imperfection diminishes and the different curves converge.

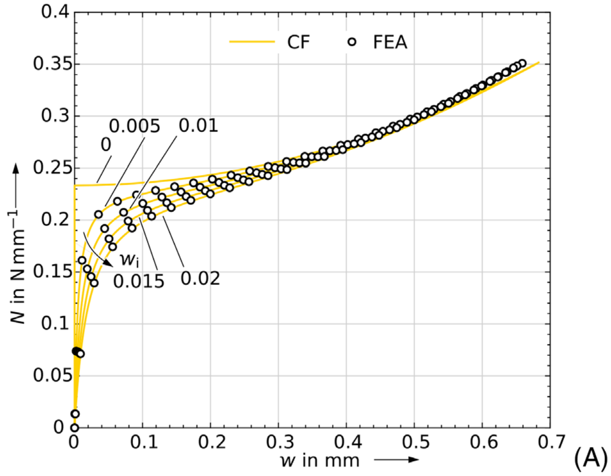

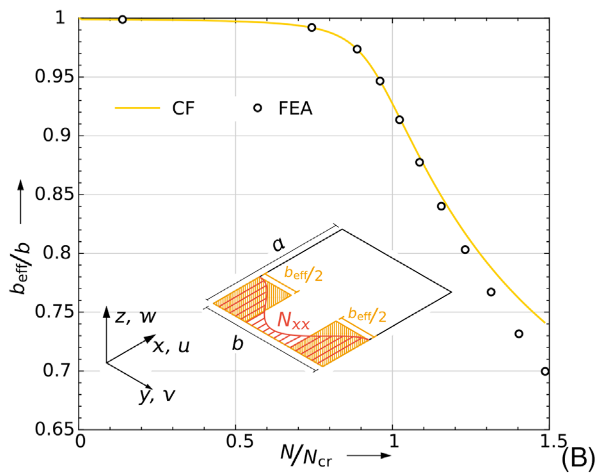

FIGURE 4 Results of the present closed-form analytical method (CF) and the FEA for the evaluation of: (A) the influence of an increasing initial imperfection w_i by investigating the load deflection behaviour; (B) the behaviour of the effective width with increasing compression.

In Figure 4B, the behaviour of the effective width computed based on the internal load distribution is illustrated taking an initial imperfection of $w_\mathrm{i} = 0.02$ into account. It can be noted that the results of the present solution show good agreement, which is very suitable for approximate methods with a deviation of only approx. 6%.

The present work proposes a novel simple closed-form analytical approximate solution for the postbuckling of shear deformable laminates. The discussed results show, that the analysis method is a computationally efficient alternative to numerical methods when the early postbuckling regime is considered. The quality of the new method is very suitable for preliminary design, where the number of function evaluations is high in the framework, for example, of an optimisation.

ACKNOWLEDGMENTS

The financial support of the German Research Foundation DFG [project number 426146527] is acknowledged with gratitude.

Open access funding enabled and organized by Projekt DEAL.

ORCID

Jakob Christian Schilling https://orcid.org/0000-0003-1611-4048
Christian Mittelstedt https://orcid.org/0000-0003-2393-4693

REFERENCES

1. Schreiber, P., Mittelstedt, C., & Beerhorst, M. (2020). Buckling of shear-deformable orthotropic laminated plates with elastic restraints. *Thin-Walled Structures*, *157*, 107071.
2. Reddy, J. N. (2004). *Mechanics of laminated composite plates and shells: Theory and analysis*. CRC Press.
3. Vescovini, R., & Bisagni, C. (2012). Single-mode solution for post-buckling analysis of composite panels with elastic restraints loaded in compression. *Composites Part B: Engineering*, *43*, 1258–1274.
4. Mittelstedt, C., & Becker, W. (2016). *Strukturmechanik ebener Laminate* Studienbereich Mechanik.
5. Beerhorst, M., Seibel, M., & Mittelstedt, C. (2012). Fast analytical method describing the postbuckling behavior of long, symmetric, balanced laminated composite plates under biaxial compression and shear. *Composite Structures*, *94*, 2001–2009.
6. Chai, G. B., Banks, W. M., & Rhodes, J. (1991). The instability behaviour of laminated panels with elastically rotationally restrained edges. *Composite Structures*, *19*, 41–65.
7. Chandra, R. (1975). Postbuckling analysis of crossply laminated plates. *AIAA Journal*, *13*, 1388–1389.
8. Mittelstedt, C., & Schröder, K.-U. (2010). Postbuckling of compressively loaded imperfect composite plates: Closed-form approximate solutions. *International Journal of Structural Stability and Dynamics*, *10*, 761–778.
9. Quatmann, M., & Reimerdes, H.-G. (2011). Preliminary design of composite fuselage structures using analytical rapid sizing methods. *CEAS Aeronaut Journal*, *2*, 231–241.
10. Beerhorst, M. (2014). *Entwicklung von hocheffizienten Berechnungsmethoden zur Beschreibung des Beul- und Nachbeulverhaltens von versteiften und unversteiften Flächentragwerken aus Faserverbundwerkstoffen* Technische Universität Berlin.

11. Schilling, J. C., & Mittelstedt, C. (2022). Local postbuckling of omega-stringer-stiffened composite panels. *Thin-Walled Structures*, *181*, 110027.
12. Beerhorst, M., & Thirusala Suresh Babu, S. (2020). Closed-form approximate solution for linear buckling of Mindlin plates with SRSR-boundary conditions. *Composite Structures*, *240*, 112037.
13. Schilling, J. C., & Mittelstedt, C. (2020). Local buckling analysis of omega-stringer-stiffened composite panels using a new closed-form analytical approximate solution. *Thin-Walled Structures*, *147*, 106534.
14. Herrmann, J., Kühn, T., Müllenstedt, T., Mittelstedt, S., & Mittelstedt, C. (2018a). Closed-form approximate solutions for the local buckling behavior of composite laminated beams based on third-order shear deformation theory. In H. Altenbach, F. Jablonski, W. H. Müller, K. Naumenko, & P. Schneider (Eds.), *Advances in mechanics of materials and structural analysis, advanced structured materials* (pp. 175–205). Springer International Publishing.
15. Herrmann, J., Kühn, T., Müllenstedt, T., Mittelstedt, S., & Mittelstedt, C. (2018b). A higher order shear deformation approach to the local buckling behavior of moderately thick composite laminated beams. *International Journal of Structural Stability and Dynamics*, *18*, 1850139.
16. Schreiber, P., & Mittelstedt, C. (2022). Buckling of shear-deformable unsymmetrically laminated plates. *International Journal of Mechanical Sciences*, *218*, 106995.

How to cite this article: Schilling, J. C., & Mittelstedt, C. (2023). Approximate postbuckling analysis of shear deformable laminates. *Proceedings in Applied Mathematics and Mechanics*, *23,* e202300082.
https://doi.org/10.1002/pamm.202300082